A LIMIT ON THE INHOMOGENEITY OF THE COSMIC MICROWAVE BACKGROUND RADIATION AT AN ANGULAR SCALE OF 1.25 ARCMIN

Thesis by

Jay Cee Pigg, Jr.

In Partial Fulfillment of the Requirements
for the Degree of
Doctor of Philosophy

California Institute of Technology
Pasadena, California

1976

(Submitted May 27, 1976)

To my patient typist and wife,

Patti

ACKNOWLEDGMENTS

The suggestions and assistance of my advisor, Alan T. Moffet, were instrumental in the decision to make these observations, in carrying out that decision, and in the writing of this paper. The Jet Propulsion Laboratory scheduled sufficient telescope time for these observations in addition to their primary task of supporting two deep space missions in progress at that time; and Roland Carpenter, Tak Sato and the staff at the telescope provided technical assistance. The author gratefully acknowledges support from a National Science Foundation Graduate Fellowship for two years and a Graduate Research Assistnatship for the remainder of his graduate studies. My reseach in radio astronomy at the Owens Valley Radio Observatory was supported by the National Science Foundation under grant MPS 73-04677, and by the Office of Naval Research, contract N00014-67-A-0094-0019.

ABSTRACT

An observational upper limit to the inhomogeneity of the cosmic background radiation of $\delta T/T \leq 7.4 \times 10^{-4}$ on an angular scale of 1.25 arcmin was obtained at a wavelength of 2.0 cm. This and Pariiskii's (1973, Astron. Zh., 50, 453 [Sov. Astron., 17, 291]) limit of $\delta T/T \leq 4.8 \times 10^{-5}$ at 22 arcmin define the observational upper limit to $\delta T/T$ for all scales 1° or less. Constraints are placed on published models of galaxy formation and 1000-Mpc scale clustering. Hypotheses that fluctuations in the background radiation could be caused by random fluctuations in the number of protogalaxies in a given solid angle, and that reionization of the intergalactic medium could be associated with the collapse of protogalaxies are shown to be consistent with the observations. Any discrete source model for the origin of the radiation would require more than 100 times as many sources as there are galaxies.

TABLE OF CONTENTS

I. INTRODUCTION

Observational limits on the inhomogeneity of the background radiation are interpreted in terms of the hypotheses that have been put forward to account for the origin of the inhomogeneity. Density (Peebles and Yu 1970) and entropy perturbations (Gott and Rees 1975) as well as turbulent motions (Chibisov and Ozernoy 1969) have been proposed to explain the formation of galaxies, and background radiation inhomogeneities would be generated at the time of recombination of the primordial plasma in all these theories. The photons could be scattered by gravitational waves propagating through the universe (Dautcourt 1969), or by an ionized intergalactic medium (Chibisov and Ozernoy 1969). The origin of the background radiation in many discrete sources spread at random throughout the sky has also been proposed (Wolfe and Burbidge 1969). All of these hypotheses predict inhomogeneity in the incident background radiation on angular scales $\leq 1^{\circ}$.

Section II of this paper describes a new observation of the cosmic background radiation made at a wavelength of 2 cm and an angular scale of 1.25 arcmin. In Section III the data are analysed to yield a limit on the inhomogeneity of the 2.7 K blackbody radiation of $\delta T/T \leq 7.4 \times 10^{-4}$, which together with previously published observations is used to set a limit on $\delta T/T$ for all angular scales $\theta \leq 1^{\circ}$.

The hypotheses advanced that predict inhomogeneity in the background are re-examined in the light of this new datum in Section IV, and a model is proposed for the scattering of the background radiation by ionized matter associated with the collapse of protogalaxies to form galaxies. Conclusions which can be drawn from this discussion are summarized in Section V.

II. DESCRIPTION OF THE OBSERVATIONS

a) Receiving System and Data Recording

Observations of the microwave background radiation were made using the 64 m (210 ft) telescope at the Goldstone tracking station, a part of the National Aeronautics and Space Administration deep space network, at a frequency of 15.3 GHz (1.96 cm) at which the telescope has a half-power beamwidth of 1.3 arcmin. The system temperature was 32 K at the zenith, and the bandwidth between half-power points was 18 MHz.

A noise-adding radiometer (NAR) injected an 81 K noise signal from an avalanche diode at 24 pulses per second with a 50% duty cycle. The receiver output was sampled and digitized, and the mean receiver temperature when the pulsed noise diode was off was calculated for each 0.2-second interval. These temperatures were written on magnetic tapes and also converted to an analog voltage displayed on a strip chart recorder. At 10-second intervals the time was written on the magnetic tape and also printed on a teletype together with the mean and standard deviation of the 50 preceding 0.2 second temperatures.

The theoretical noise level of the NAR is given by Nicolson (1970) as

$$\delta T = 2\, T_o\, (1 + T_o/T_n) \,/\, (bw \cdot t)^{\frac{1}{2}} \qquad (1)$$

which for t = 1 second gives 21 mK. The typical observed 1-second noise level in good weather above zenith angles of

50° was 27 mK.

A second teletype printed the times at which commands were issued to the tracking system, and a third teletype printed the telescope hour angle and declination continuously at 10-second intervals.

b) Method of Observation

A region in Pegasus extending 105^{s} from $23^{h}44^{m}43^{s}$ to $23^{h}46^{m}28^{s}$ (1950.0) at a constant declination of $16^{\circ}01'.8$ with a width of one beamwidth was selected to avoid nearby galaxies, the central regions of known clusters of galaxies, and known radio sources. Approximate galactic coordinates are $\ell = 102^{\circ}$, $b = -44^{\circ}$.

The telescope scanned the selected region continuously at $\pm$ the sidereal rate; with respect to the ground the telescope was alternately stationary and moving west at twice the sidereal rate. This procedure was chosen to minimize the relative error between antenna temperatures measured at different points within the selected region, such as errors caused by receiver gain changes or time-varying contributions to the antenna temperature (e.g. changes in the water vapor content of the air, or changes in the elevation angle of the telescope).

Table 1 lists the dates observations were made, together with the time spent on the selected region, the average one-second noise level, the weight adopted in the averaging process, the number of scans made, the effective

number of scans (number of scans times the weight), and the zenith angle range of the observations. Each hour the nearby source 3C454.3 and a 3.6 K noise calibration were observed as a check on the pointing and gain of the system.

TABLE 1

SUMMARY OF OBSERVATIONS

Date	On-source Time	1-sec. Noise	Weight	Scans	N_{eff}	Zenith Angles
29 July 74	3.6 hr	117 mK	0.15	107	15.7	19-59°
31 July 74	2.9	31	2.13	86	183.6	19-45
2 Aug. 74	2.6	48	0.85	78	66.5	21-34
20 Feb. 75	3.0	51	0.77	90	69.4	39-82
23 Feb. 75	2.9	43	1.10	87	96.0	43-79
14 Mar. 75	2.5	315	0.02	74	1.5	53-81
Total	17.4 hr	49 mK	0.83	522	432.7	19-82°
First 5 days only	14.9 hr	46 mK	0.96	448	431.2	19-82°

c) Calibration

The NAR pulsed diode was the standard for all the observations; its temperature was measured by comparison with a load at ambient temperature before each day's observations.

The aperture efficiency of the antenna was 22.4 ± 1.4% at 45° zenith angle, based on the observation that 3C454.3 produced an antenna temperature of 3.3 ± 0.2 K on July 31, 1974, at which time it had a flux at 15 MHz of 12.6 ± 0.2 Jy (Dent and Kapitzky 1975).

The aperture efficiency measures the response of the antenna to a point source; the response of the antenna to a source that fills the main beam is the beam efficiency. At 15 GHz the moon is a thermal source with a brightness temperature at the center of the disk of (Troitsky 1962; Linsky 1973)

$$T_{moon} = 240 + 25 \cos (i-40^{\circ}) \pm 10 \text{ K}. \qquad (2)$$

where i is the phase angle (i=0 at full moon). On February 20, 1975, the antenna temperature at the center of the lunar disk was observed to be 112.8 ± 0.1 K at which time the expected brightness temperature of the moon was 224 ± 10 K; the beam efficiency was therefore 48 ± 2 %.

At 15.3 GHz the Rayleigh-Jeans approximation, in terms of which antenna temperatures are defined, overestimates a 2.73 K blackbody intensity by a factor of 1.15. However, the slope of the approximation differs from the slope of

the blackbody intensity curve by less than 1%. Small differences in the blackbody brightness temperature would therefore produce the same differences in antenna temperature within 1% (in the case of 100% beam efficiency), and no correction for the Rayleigh-Jeans approximation is made in this paper.

d) Atmospheric Effects

When the antenna is tipped away from the zenith, refraction by the atmosphere causes an apparent displacement of the source, and the antenna temperature rises because of the increased path length through the atmosphere. The necessary refraction correction was made by the telescope pointing program.

The antenna temperature at zenith in 1974 was 28 K, but in 1975 was 32 K because of modifications to the receiving system made at the end of 1974. Figure 1 is a plot of the antenna temperature as a function of the zenith angle of the telescope and as a fuction of the secant of the zenith angle, which is proportional to the path length through the atmosphere. The antenna temperature increased 4.55 K with each unit increase in the secant for zenith angles greater than 60°. Values from 1974 have been increased by 4 K in Figure 1. No observations were made at zenith angles less than 19°.

The one-standard-deviation radiometer output noise fluctuations for one second of integration time were

approximately equal to the antenna temperature times 10^{-3}.

Water vapor in the atmosphere can make large contributions to the antenna temperature at 15 GHz. On March 14, 1975, at a time when the sky was heavily overcast, an antenna temperature which exceeded the value expected from Figure 1 by more than 12 K was observed at a zenith angle of 61°. Moreover, as the telescope beam was in motion with respect to the clouds, rapid changes in antenna temperature occurred with amplitudes of several degrees Kelvin. Even at some times when no clouds were visible in the telescope beam the one-second noise level was as much as a factor of two above the value expected from Figure 1. This was attributed to inhomogeneity in the water vapor distribution in the atmosphere as it moved through the telescope beam.

The large differences in the noise level of the antenna temperature at different zenith angles and under different weather conditions required that a weighting procedure be used to obtain the maximum-likelihood average scan.

III. DATA ANALYSIS

a) Data Reduction

The data reduction included the following steps: alignment, baseline removal, weighting, and averaging. The region observed was analyzed by considering it to consist of 21 cells of solid angle equal to the half-power beam of the antenna (1.25 arcmin in diameter). Five seconds of integration time were obtained in each cell during each scan.

The time and coordinates of each telescope motion reversal were obtained from the continuous position printout; physical reversal occurred 2 seconds after the command was issued. The times at which the telescope beam had entered and left the selected region were computed, then the five 0.2-second antenna temperature measurements corresponding to each second of right ascension in the selected region were identified, averaged, and stored for the next step in the reduction. The accuracy of the alignment procedure was obtained from the observations of 3C454.3; in 58 scans the right ascension of the peak antenna temperature had a scatter of 1.2 seconds = 0.3 arcmin (one standard deviation).

The component of the antenna temperature which was a function of zenith angle was then removed by subtracting a linear baseline from each scan.

To assign weights to the data, each hour of observations was treated as a block. The approximately thirty scans were averaged, cell by cell, to form a "mean scan". By standard statistical methods (Bennett and Franklin 1954) the variance of the data corrected for the mean of each scan and of each cell in the mean scan was calculated. The reciprocal of this variance times 0.002 was the weight used for that hour when averaging over all hours of observations. The constant 0.002 was chosen to make the weights sum to approximately the number of scans (neglecting March 14 scans); it corresponds to a one-second noise level of 44.7 mK. The average weight for each day is shown in Table 1.

The very low weight for March 14, 1975, was due to a heavily overcast sky. The data from March 14 were not used in the final averaging procedure. The mean scan resulting from the weighted average of all 448 scans obtained on the first five days is graphed in Figure 2.

The one-second noise level of all the data, corrected for the mean of each scan and of each cell in the mean scan, was 45.5 mK. This corresponds to a standard deviation of 0.96 mK when integrated for 2240 seconds; the observed standard deviation of a cell in the mean scan is 0.95 mK. In order for the differences between the cells significantly to exceed the random noise in this experiment, the standard deviation (squared) of a cell in the mean scan

would have had to be $(0.96\ \mathrm{mK})^2 \times 1.57 = (1.20\ \mathrm{mK})^2$, where 1.57 is the F ratio at the 95% confidence level.

An upper limit to the variance due to possible cell-to-cell sky brightness temperature variations that might be masked by noise can be computed from the formula (Bennett and Franklin 1954):

$$L^2(p) = \frac{(F - F(n_1, n_2, 1-p))}{F(n_1, \infty, 1-p)} \quad \frac{s^2}{n} \qquad (3)$$

where L^2 is the upper limit to the variance at a confidence level p, $F = (0.95/0.96)^2$ is the ratio of observed variances, $n_1 = 20$ and $n_2 = 8940$ degrees of freedom, and $s^2/n = (0.96\ \mathrm{mK})^2$ as derived above. Values of L at several confidence limits are given in Table 2, under the heading "Statistical Method."

TABLE 2

UPPER LIMIT TO COSMIC BACKGROUND VARIATIONS.

Confidence Level	Statistical Method		Graphical Method	
	δT_A	δT_B	δT_A	δT_B
50%	0.12 mK	0.45 mK	0.0 mK	0.0 mK
90%	0.73	2.75	0.47	1.77
95%	0.86	3.24	0.53	2.00*
97%	0.95	3.58	0.57	2.15
99%	1.13	4.26	0.63	2.38

δT_A refers to antenna temperature, δT_B refers to sky brightness temperature on an angular scale of 1.25 arcmin.

*indicates the value adopted for discussion in this paper.

b) Analysis by the Graphical Method

In the preceding section, the scatter in the data due to inhomogeneities in the sky brightness temperature was separated from that due to receiver noise and atmospheric effects by grouping observations of the same point on the sky made at different times and by applying standard methods of statistical analysis which compare the variance between groups with the variance within groups. This procedure, to which this paper will refer as the "statistical" method, was used by Carpenter et. al. (1973). An alternative analysis of the data, which might be called the "graphical" method, was used by Conklin and Bracewell (1967b) and by Pariiskii (1973c).

In a mean scan constructed by averaging n scans together, the random component of the variance is 1/n times the random component of a single scan, but the fixed component remains unchanged. The graphical method consists in fitting the observed variances of mean scans which are averages of different numbers of scans by a linear equation of the form:[1]

---

[1] It would not be equivalent to do a linear fit on the standard deviation of the form $s(n) = s_1 n^{-\frac{1}{2}} + a$ because that implies $s^2(n) = s_1^2 n^{-1} + 2 s_1 n^{-\frac{1}{2}} a + a^2$. Since there is no cross product in the correct relation, the fitting procedure would be forced to give a value for "a" significantly smaller than s_s. When such fits were made to the mean scans actually used in Figure 2, values of a from $0.5\ s_s$ to $0.1\ s_s$ were obtained.

$$s^2(n) = s_1^2 n^{-1} + s_s^2. \qquad (4)$$

The $n^{-1} = 0$ intercept is then the estimated antenna temperature mean-square fluctuation due to non-atmospheric brightness temperature differences from point to point on the sky.

The upper limit to s_s at a given confidence level depends on the accuracy of the points fitted; in addition to values of $s^2(n)$, the standard deviations of those values must be estimated. Conklin and Bracewell did this by comparing data from different hours; an analogous procedure was used in this paper.

Conklin and Bracewell accumulated scans in the order in which they were obtained to calculate mean scans corresponding to 1,4,10,16,25, and 36 days. The data presented in this paper varied so much in noise level from day to day (see Table 1) that a different scheme was required: scans were included from all five days of observing in each mean scan.

The solid points in Figure 3 refer to the mean, and one standard deviation of the mean, of the variances of 448/n mean scans, each obtained by averaging n scans.[2] Thus each scan contributes once to each point. Since there are 20 x 447 degrees of freedom available, each point remains statistically independent and is at the same time as well determined as possible given the available data.

---

[2] The standard deviation for n = 448 was estimated by comparison with other n's.

For comparison open points are also plotted for 3 mean scans each of 112, 28 and 7 scans, and seven single scans. Thus each scan contributes once only.

Least-squares fits were made to Equation 4 for the solid points and for the open points independently. The fit to the solid points is shown in Figure 3, and the coefficients of both fits are given in Table 3. The one-second noise calculated from the slope of the fit to the solid points is in excellent agreement with the 46 mK average for the first five days from Table 1. The fit to the solid points was used to calculate the limit in Table 2;[3] at the 95% confidence level the graphical method gives 0.53 mK (2.00 mK after the corrections for beam efficiency and angular scale factor), and in general all the graphical limits are about 0.6 times the corresponding statistical limits.

This discrepancy might be due in part to the additional constraint of Equation 4, which allowed the data to be extrapolated beyond n = 448 scans. Also, Figure 3 shows that the variance of the 448-scan mean scan —which determines the statistical method limit— is greater than the fit to all the solid points at n = 448.

---

[3] The negative value of the intercept was replaced by zero in this calculation.

TABLE 3

COEFFICIENTS OF FITS TO EQUATION 4

	Solid Points	Open Points
s_1^2	426.5 ± 6.7 mK^2	333.0 ± 25.8 mK^2
$s_1\sqrt{5}$	46.2 mK	40.8 mK
s_s^2	-0.220 ± 0.173 mK^2	0.371 ± 0.486 mK^2
$\lvert s_s^2 \rvert^{\frac{1}{2}}$	0.47 mK	0.61 mK

Figure 2 shows that the maximum antenna temperature occurred in cell 19, which is 2.5 standard deviations from the scan mean. A Gaussian-distributed random variable has a probability of 1.2% of falling farther than 2.5 standard deviations from the mean. The instantaneous response of the antenna to a hypothetical source of 15 mJy located between cells 19 and 20 has been drawn in Figure 2 together with the adjusted baseline, a least-squares linear fit to the residuals. The open circles indicate the antenna temperature due to the hypothetical source averaged over each cell. A 15 mJy source has a 24% probability of occurring in the observed region. If the contribution of the hypothetical source is removed, the standard deviation of the 21 residuals becomes 0.64 mK instead of 0.95 mK (0.57 mK after the contribution of many faint sources is subtracted as in the next paragraph). The limit on the inhomogeneity of the cosmic background would be reduced, and would agree with the result of the graphical analysis, which has therefore been adopted in this paper: 0.53 mK at 95% confidence.

To obtain the limit on sky brightness temperature fluctuations, the limits on antenna temperature fluctuations in Table 2 must all be divided by 0.48 to correct for the beam efficiency and multiplied by an angular scale function to correct for the convolution of the sky brightness distribution with the antenna beam as discussed below.

The adopted limit at 1.25 arcmin after these corrections is 2.00 mK, which is 0.74×10^{-3} times the background radiation temperature of 2.7 K.

c) Confusion by Faint Sources

Extrapolation of the integral number-flux density curves of Wall and Cooke (1975) from 2.7 and 5 GHz to 15 GHz indicates unit probability that a source stronger than 3.6 mJy would occur in a solid angle equal to the selected region (3.1×10^{-6} sr), and that the relationship from $10^{4.5}$ to 10^{6} sources/sr can be approximated by $N = N_o (S/S_o)^{-1}$. A 3.6 mJy source would make a maximum antenna temperature contribution of 0.94 mK and a maximum contribution to the average temperature in one cell of 0.78 mK. If for simplicity one assumed that within the selected region there was one source contributing 0.8 mK, one of 0.8/2 mK, one of 0.8/3 mK, and so forth, and that the variance contributed by each was additive, then the sum of all such sources[4] would cause a standard deviation of 0.23 mK[5] between cells in the

---

[4] In this simple model the total variance is $0.64\pi^2/6$ mK^2 and the variance of one cell is that divided by 21. The average antenna temperature sums to $0.8\ (\ln(n)-0.6)/21$; for n = 200 sources in the selected region this is only 0.18 mK per cell. The model is inapplicable for $n \gg 21$ sources because the sources would not contribute additively to the variance between cells. The 15 mJy source suggested in the previous paragraph does not enter this estimate.

[5] A 0.9 mJy source would cause a maximum antenna temperature of 0.23 mK, and would have unit probability of occurring in a solid angle of five times the half-power beam.

absence of noise and cosmic background fluctuations. This value is represented by a circle in Figure 4. Subtracting it in quadrature from the observed standard deviation between cells leaves 0.91 mK, a decrease of 4%. In other words, the limit derived by this paper is not strongly affected by confusion from many sources all weaker than the receiver noise level.

If the observed sky brightness temperature fluctuations arise entirely from discrete sources, they imply a source number-flux density relationship: one source per beamwidth solid angle with a flux equal to the sky fluctuations (Longair and Sunyaev 1969). This yields 6.8×10^6 sources/sr with a flux of 1.6 mJy, which is a factor of 30 above the number at that flux found by Wall and Cooke at 5 GHz and 20 times the number found by Pariiskii (1973b) at 7.5 GHz. Therefore, such discrete sources cannot be the cause of most of the observed antenna temperature fluctuation.

d) Extrapolation to Other Angular Scales

This measurement of the inhomogeneity of the cosmic microwave background radiation made at 1.25 arcmin implies limits at other angular scales. Conklin and Bracewell (1967b) find that, for an antenna with a Gaussian pattern and half-power beamwidth W, the implied limit on the root-mean-square fluctuations with "angular scale" θ is given by

$$\delta T_B(\theta) = (1 + (1.51\ W/\theta)^2)^{\frac{1}{2}}(s_s/\eta) \text{ for } \theta \leq 1.51\ W \quad (5)$$

and, in particular,

$$\delta T_B(W) = 1.81\ s_s/\eta \quad (5a)$$

where $\eta = 0.48$ is the beam efficiency and $W = 1.25$ arcmin. The "angular scale" is defined as the first moment of the two-dimensional spatial autocorrelation function of the sky brightness temperature distribution, which is assumed to be independent of orientation.

The limit on fluctuations with angular scale larger than the telescope beamwidth can be obtained by integrating the data to simulate a wider beam; Equation 5 is replaced by:

$$\delta T_B(\theta) = (3.02\ W/\theta)^{\frac{1}{2}}\ (s_s/\eta) \quad \text{for } \theta \geq 1.51\ W. \quad (6)$$

Thus the angular scale correction factor is greater than unity for all angular scales less than three beamwidths.

The 448-scan mean scan was roughly corrected for the contribution in each cell of radiation incident in the wings of the main beam from adjacent cells by the formula

$$T'(n) = (\ 5\ T(n) - T(n-1) - T(n+1)\ )\ /\ 3.$$

The corrected antenna temperatures are shown in Figure 2 as solid points. The standard deviation of the corrected antenna temperatures was 1.50 mK, corresponding to $s_s = 0.40$ mK in Equation 5a. When adjacent cells were then averaged to simulate wider beams up to $\theta = 6\ W$, the observed fluctuations were within 5% of the values predicted

by Equation 6. When the uncorrected cell temperatures were averaged similarly, the derived fluctuations exceeded the $\theta^{-\frac{1}{2}}$ law and approached the values for the corrected data because the uncorrected temperatures are not completely independent.

Figure 4 shows the limit on sky brightness fluctuations as a function of angular scale; the value 0.53 mK was used for s_s. The curve can be approximated by the following asymptotic forms:[6]

$$\delta T_B \ (\theta \leq 0.4 \text{ arcmin}) = 2.1 \ \theta^{-1} \text{ mK} \qquad (7a)$$

$$\delta T_B \ (\theta \geq 1.5 \text{ arcmin}) = 2.1 \ \theta^{-\frac{1}{2}} \text{ mK} \qquad (7b)$$

Figure 4 also shows the limits obtained by other observers; the wavelengths and references are listed in Table 4. The dashed line indicates the locus of possible observations that would extrapolate to 2.0 mK at 1.25 arcmin.

The region observed was only 26.25 arcmin in extent; consequently, the extrapolation of this measurement to angular scales greater than 20 arcmin is unjustified.

---

[6] In general $\delta T_B(\theta \leq W/3) = 0.83 \ \delta T_B(W) \ (\theta/W)^{-1}$ and $\delta T_B(\theta \geq 1.2W) = 0.96 \ \delta T_B(W) \ (\theta/W)^{-\frac{1}{2}}$. Note that an observation made by beamswitching (or integrating a scan) an angular distance W' of three or more half-power beamwidths has $\delta T_B(W') = s_s/\eta$ and extrapolates according to the same equations with W replaced by W'. (See Table 4.)

Each of the observational points in Figure 4 can be extrapolated; together they define a lowest limit at every angular scale $\theta \leq 1^{\circ}$. The envelope so produced is equal to Pariiskii's (1973a = P1) limit at 22 arcmin (δT = 0.13 mK) and its extrapolation for $\theta \geq 1.75$ arcmin and the limit set in this paper (δT = 2.0 mK at θ = 1.25 arcmin) with its extrapolation for $\theta < 1.75$ arcmin.

TABLE 4A

LIMITS ON COSMIC BACKGROUND FLUCTUATIONS

PLOTTED IN FIGURE 4

Label	Beam-width[a] (arcmin)	Angular Scale (arcmin)	Upper Limit (mK)	Wave-length (cm)	Method[b]
BP	1.3	3.0	4.3[c]	0.35	2s
CB1	12	60	5.1	2.8	1g
CB2	12	12	4.8	2.8	1g
CGS	2.3	2.3	1.90[d]	3.6	1s
E	3	60	30[c]	0.34	2
JCP	1.3	1.25	2.00	2.0	1g
P1	1.3 x 40	22.4[e]	0.13	4.0	1g
P2	2.8	6	0.48	2.8	2g
	and	60	0.48		
PP	1.4 x 20	10.6[f]	0.7	4.0	2g
PSW	1.1	2.2	40[c]	0.35	1r
PW	40	40	6[c]	0.35	1r
S	6	6	2.9	11.1	1r

[a] Beamwidth to half-power points.

[b] (1), Continuous scanning with the data integrated to the angular scale indicated; (2), Beamswitching; (s), The data were analysed by the statistical method; and (g), By the graphical method; (r), The root-mean-square scatter of data, corrected for beam efficiency but not for receiver noise or angular scale factor, is taken as the upper limit on δT_B.

[c] 0.35 cm is outside the Rayleigh-Jeans region;

$\delta T/T = \delta T/1.15$ K. See section IV a.

[d] 1.05 mK x 1.81 angular scale factor.

[e] 12.5 x 40 arcmin.

[f] 5.6 x 20 arcmin.

TABLE 4B

REFERENCES TO LIMITS

PLOTTED IN FIGURE 4

Label	Original Reference		Revised in	
BP	Boynton and Partridge	1973		
CB1	Conklin and Bracewell	1967a		
CB2	Conklin and Bracewell	1967b	Smith and Partridge	1970
CGS	Carpenter *et. al.*	1973	this paper	
E	Epstein	1967		
JCP	this paper			
P1	Pariiskii	1973a		
P2	Pariiskii	1973c	Pariiskii	
PP	Pariiskii and Pyatunina	1970		
PSW	Penzias *et. al.*	1969	Smith and Partridge	1970
PW	Penzias and Wilson	1966	Penzias *et. al.*	1969
S	Stankevich	1970	Cf. extrapolation to $\theta = 1.^{o}2$ Sunyaev and Zeldovich 1970b	

IV. CONSTRAINTS PLACED ON COSMOLOGICAL MODELS

We now re-examine a number of hypotheses concerning the generation of inhomogeneity in the cosmic background radiation in the light of this new limit. To compare numerically the minimum $\delta T/T$ at each angular scale as described in the preceding paragraph with the $\delta T/T$ estimated in papers discussing the various hypotheses, three cosmological parameters must be known. In this paper Einstein's constant Λ is assumed to be identically zero. The Hubble expansion parameter H_o is taken as 55 km s^{-1} Mpc^{-1} = $(1.8 \times 10^{10} yrs)^{-1}$ following Sandage and Tammann (1975). The corresponding density of the Einstein-deSitter universe is $\rho_c \equiv 3 H_o^2/8\pi G = 6 \times 10^{-30}$ g $cm^{-3} = 9 \times 10^{10}$ $M_\odot$ Mpc^{-3}. The density parameter $\Omega \equiv \rho/\rho_c$ is about 0.1 (Gott *et. al.* 1974; Gott and Rees 1975; Peimbert and Torres-Peimbert 1976) The symbol $\bar{\Omega} \equiv \Omega/0.1 \approx 1$ (Omega-bar) is defined to indicate the dependence of various quantities on the density of the universe in conjunction with numerical values computed for the case $\Omega = 0.1$. With this choice of parameters a spherical volume containing 10^{15} $M_\odot$ has a diameter $60\bar{\Omega}^{-1/3}$ Mpc today and subtends an angle of $1.9\bar{\Omega}^{2/3}$ arcmin when observed at a redshift of $z = 10^3$. The symbol $M_{15} \equiv M/10^{15}$ $M_\odot$ is defined for convenience.

The hypotheses that will be discussed are: (a) scattering in the reionization era, (b) density perturbations, (c) large-scale density perturbations, (d) phase

effects on acoustic perturbations, (e) discrete sources, (f) a protogalactic scattering model, (g) entropy fluctuations, (h) primordial turbulence, and (i) interactions with gravitational waves.

a) Scattering in the Reionization Era

The perturbations of the cosmic background radiation are dominated by the conditions at the epoch of its last scattering by matter. If all of the matter were in the form of a homogeneous, fully ionized plasma, its optical depth would be $\tau_i = \Omega^{\frac{1}{2}} \approx 1$ at a distance given by $z = 22$ (Chibisov and Ozernoy 1969). However, if reionization of the gas[7] were caused by processes associated with the initial collapse of galaxies at $z = 8$,[8] then the optical depth is $0.23\Omega^{\frac{1}{2}}$, and the smoothing of perturbations generated during the earlier recombination era by the reionized gas is insignificant. Sunyaev and Zeldovich (1970a) similarly conclude that for a variety of possible histories of the intergalactic gas its optical depth is less than two, and fluctuations would be smoothed by less than one order of magnitude.

---

[7] A period of neutral hydrogen in the evolution of the universe is unavoidable. Reionization is postulated to account for the failure to observe intergalactic HI and to provide a hot gas as a source of the soft X-ray background (Zeldovich and Sunyaev 1969).

[8] Epoch of maximum expansion (Cf. Gott and Rees 1975). Fuller discussion below in conjuction with "discrete scatterers" model.

In the event that the optical depth of the reionized gas were of order unity, perturbations in the density, motion and rate of heating of the gas might have generated fluctuations in the background radiation greater than those originating at larger redshifts. For example, Silk (1974b) calculates the temperature fluctuations caused by shear motions generated by mutual tidal torques between density fluctuations capable of forming bound systems by the present epoch. He finds that $\delta T/T$ is independent of scale for $M_{15} \leq 1$ ($\theta \leq 5.5$ arcmin at $z = 30$, the epoch of last scattering). The predicted fluctuations exceed the observational limits at 5.5 arcmin unless Ω exceeds 0.6, which is inconsistent with the observed pregalactic helium abundance unless $H_o \leq 20$ km s^{-1} Mpc^{-1} (Peimbert and Torres-Peimbert 1976). It appears that the assumption of optical depth comparable to unity at redshifts $z \ll 10^3$ is excluded.

b) Density Perturbations

The dominant contribution to fluctuations in the radiation temperature by density perturbations in the recombination era is from Thomson scattering by moving electrons. Silk (1974b) calculated that $\delta T/T$ increases with decreasing mass[9] until 10^{14} $M_\odot$ ($0.8\Omega^{-\frac{1}{2}}$ arcmin), below which the temper-

[9] Silk used a power spectrum of density perturbations independent of scale because this was inferred by Peebles (1974) from the spatial correlation of galaxies. Gott and Rees (1975) argued that a more correct interpretation of Peebles' data would be an $M^{-1/3}$ spectrum, but Silk's conclusions would not be greatly modified because his normalization was taken close to the mass scale of interest.

ature fluctuations are rapidly lost due to the increasing optical depth to the redshift at which smaller regions become transparent. At the peak the predicted fluctuations exceed the limit reported in this paper unless Ω exceeds 0.16.

Sunyaev and Zeldovich (1970a) have used similar arguments with a different normalization, a different mass spectrum, and a steeper dependence of optical depth on mass to predict fluctuations much smaller in amplitude than Silk calculated. They argued that, on scales smaller than the Jeans mass,[10] the amplitudes of adiabatic perturbations were multiplied with no increase in the velocity perturbations during the transition from the acoustic mode to the growing mode. The density and associated velocity fluctuations required to produce today's astronomical objects were consequently smaller at recombination than would otherwise be expected by a factor ranging from unity at the Jeans mass to 16 at 10^{15} $M_\odot$ and 200 at 10^{11} $M_\odot$ ($\Omega = 0.1$).

---

[10] The Jeans mass is the density times the volume of a sphere of diameter equal to the Jeans length, which is the characteristic scale at which positive density perturbations in the gas become unstable to gravitational collapse to bound systems.

c) Large-scale Density Perturbations

The cosmic background radiation observations set a limit on the density perturbations today on scales larger than the Jeans length just before recombination,[11] $M_{15J} = 125\Omega((\Omega+1)/2)^{-3}$ ($\theta_J = 9.4\Omega((\Omega+1)/2)^{-1}$ arcmin, $L_{oJ} = 300\ ((\Omega+1)/2)^{-1}$ Mpc.). At $\theta = 9.4$ arcmin the observations imply $(\delta\rho/\rho)_o < 1.65\Omega^{-1/6}$, and at $\theta = 22$ arcmin ($L_o = 700\Omega^{-1}$ Mpc) $(\delta\rho/\rho)_o < 0.3\Omega^{-1/6}$ (Sunyaev and Zeldovich 1970a).

A simplified model, predicting larger temperature fluctuations for a given density fluctuation, would require even lower limits on large-scale clustering. For an adiabatic perturbation $\frac{\delta T}{T} = \frac{1}{3}\left(\frac{\delta\rho}{\rho}\right)_{rec} e^{-\tau}$, where $\tau = 0.4$ for $M_{15} >> 1$ and $\tau = 1$ for $M_{15} = 1.6$ (Sunyaev and Zeldovich 1970a); and the largest possible linear growth factor for density perturbations in an $\Omega = 0.1$ universe from the recombination era to the present epoch is 70 (Gott and Rees 1975). The resulting limits are displayed in Table 5.

---

[11] The Jeans length after recombination contained only $10^5 M_\odot$—typical of a globular star cluster (Sunyaev and Zeldovich 1970a).

TABLE 5

UPPER LIMIT OF DENSITY ENHANCEMENT AT LARGE SCALES

Angular Scale ($z = 1000$) (arcmin)	Present Diameter (Mpc)	Mass Contained (10^{15}) Solar Masses	Observed Temperature Fluctuation ($\delta T/T$) Upper Limit	Present Epoch Density Fluctuation $(\delta\rho/\rho)_o$ Upper Limit
2.2	$70\Omega^{-1}$	$1.6\Omega^{-2}$	4.1×10^{-4}	0.23
6	$200\Omega^{-1}$	$32\Omega^{-2}$	1.8×10^{-4}	0.056
9.4	$300\Omega^{-1}$	$125\Omega^{-2}$	1.12×10^{-4}	0.036
22	$700\Omega^{-1}$	$1600\Omega^{-2}$	4.8×10^{-5}	0.0153
31	$1000\Omega^{-1}$	$4500\Omega^{-2}$	4.1×10^{-5}	0.0130

Silk (1974a) points out that, for a system to be destined to recollapse in the future, $(\delta\rho/\rho)_0$ must be $\geq 4\Omega^{-1}$, since the linear growth of small density perturbations ended at $z = \Omega^{-1}$.

The departures to be expected from the Hubble expansion velocity have been calculated by Silk (1974a) and can be approximated by $(v/r)/H_0 = 0.2\ (\delta\rho/\rho)_0 \Omega^{-2/3}$. Therefore $(\delta\rho/\rho)_0 \leq 0.35\Omega^{2/3}$ is implied by the observations of Weedman (1976), who found a scatter of $\leq 7\%$ from the Hubble law in the velocities of clusters at distances of 20 to 220 Mpc. Webster (1976) found that radio galaxies are unclustered; on scales of 150 Mpc or more $(\delta\rho/\rho)_0 \leq 10\%$.

d) Phase Effects on Acoustic Perturbations

Density pertubations on scales less than the Jeans mass just before recombination (cf. preceding paragraphs) oscillated as acoustic waves for an interval of time preceding recombination. If recombination had occurred at the time that the velocity of the matter was zero, the density perturbation would grow very slowly and would contribute very little to the inhomogeneity of the background radiation. Sunyaev and Zeldovich (1970a) estimate that the transition from the acoustic mode to the linear growth mode occurs rapidly enough for this to happen, and that the angular scales at which $\delta T/T$ might be expected to be near-zero are $\theta_0(n) = \theta_J/((n + \frac{1}{2})\pi - \phi)$, where $n = 0,1,2,3,\ldots$ and ϕ is a constant. For $\Omega = 1$ and $\phi = 0$, the first four θ are

6.0, 2.0, 1.2, 0.35 arcmin.

Coincidentally the first three θ_o are the angular scales of the observations labelled P2, CGS, and JCP (this paper) in Figure 4 and Table 4. In order for P1 at 22 arcmin to be affected, however, either A or ϕ must be large. No choice of the parameters with A positive can invalidate both the 22 and 6 arcmin observations; hence, at worst, the upper limit on $\delta T/T$ would be increased by a factor of $(22/6)^{\frac{1}{2}} \approx 2$ for angular scales greater than 6 arcmin. Moreover, the spacing in angular scale between successive minima of $\delta T/T$ would be a factor of three or less. Since pencil-beam observations have a wider angular frequency bandpass than that, an observation made at the scale of a minimum would still detect the next maximum.

e) Discrete Sources

The effect of confusion on the determination of the fluctuations in the background radiation was discussed in a previous section. Some authors, e.g. Wolfe and Burbidge (1969), have proposed that the background radiation itself is due to unresolved discrete sources rather than to an early, hot compact stage of evolution of the universe. Smith and Partridge (1970) have calculated limits on the basis of the most general and conservative assumptions, and they included the effects of scattering by an intergalactic plasma. If the sources are assumed to spread back in time from when the universe was 10^8 years old ($z \approx 50$)

down to the epoch z_o ($0 \leq z_o \leq 40$), the minimum number of sources required to make the background as smooth as observed in this paper is 5.8 sources per Mpc^3, more than 100 times the density of galaxies.

Another argument against the discrete source hypothesis for the origin of the background radiation is the fact that the thermal spectrum is very difficult to reproduce. In fact, the superposition of spectra from single sources can produce a spectrum of the blackbody type if and only if they are in equilibrium with the evolutionary temperature $T_o(1 + z)$ (Alexanian 1970). Thermalization of sources, for example by dust, down to wavelengths longer than 21 cm is very difficult to contrive (Layzer and Hively 1973). It is now known that the spectrum of the background radiation closely follows the 3^oK Planck function which would be impossible to simulate with spectra of known discrete sources (Woody et. al. 1975).

The discrete source hypothesis is the only one advanced by proponents of the steady-state cosmologies, and the combination of a 3^oK Rayleigh-Jeans spectrum, which is not observed in any known discrete source, and the homogeneity of the radiation— which required source densities comparable to the number density of galaxies to fit the observations published by 1970— has apparently ruled out the steady-state cosmological models (Smith and Partridge 1970).

f) A Protogalactic Scattering Model

An alternative to the discrete source model could be the following "discrete scatterers" model. Galaxies with a free-fall collapse time t_{ff} reach their maximum extent at $t_{cosm} = t_{ff}$, collapse to a minimum diameter at $t_{cosm} = 2\ t_{ff}$, and re-expand to approximately half their maximum extent, becoming approximately virialized by $t_{cosm} = 3\ t_{ff}$. For a galaxy of $2 \times 10^{11} M_{\odot}$, $t_{ff} = 1.1 \times 10^{9}$ yrs (Gott and Rees 1975), and the redshifts corresponding to the three critical epochs mentioned are $z_{max} = 8$, $z_{min} = 5$, $z_{vir} = 3.8$. If all the matter were in the form of ionized gas throughout the era considered, the optical depth to the observer from those redshifts would be $\tau(8) = 0.23\Omega^{\frac{1}{2}}$, $\tau(5) = 0.12\Omega^{\frac{1}{2}}$ and $\tau(3.8) = 0.08\Omega^{\frac{1}{2}}$ (Chibisov and Ozernoy 1969). The galaxies would scatter the background radiation unequally along different lines of sight because of random inequalities in the number of galaxies along different lines of sight. The angular scale involved corresponds to the distances between galaxies, not their physical diameters, and is 0.94, 1.39 and 1.69 arcminutes at the critical epochs. Therefore comparison with the observation reported in this paper at 1.25 arcmin requires only a one-dimensional model.

The number of scatterers in the line of sight is $N = c\delta t / L(z)$, where δt is the time interval during which

this scattering was effective and $L(z) = 4.47\Omega^{\frac{1}{2}}(1+2)^{-1}$ Mpc. is the spacing between galaxies. If the scattering became effective (reionization occurred) at $z \approx 8$ and ended at $z \approx 3.8$ (most of the gas condensed into stars) then $N \approx 1200$, and $N^{-\frac{1}{2}} = 0.03$. If $\delta T = N^{-\frac{1}{2}} \tau\ (2.7\ K) \leq 2$ mK, then τ, the opacity averaged over many lines of sight, is ≤ 0.016. If the scattering is effective from $z \approx 5$ to $z \approx 3.8$, then $N \approx 450$, $\tau \leq 0.026$. The required optical depth in each case is less than the predicted optical depth.

The area of a galaxy decreases from 0.30 times the distance between galaxies at $z = 8$ to 0.023 at $z = 4$. Probably some ionized gas would still not have fallen into the galaxies by $z = 4$, so the optical depth of the matter would not decrease as dramatically as the area. Moreover, until the galaxies became optically thick, their efficiencies as scatterers would be nearly independent of their degree of condensation, provided the gas remained ionized at all times.

The advantages of the protogalactic scattering model over the discrete sources model are: (1) the blackbody spectrum is primordial rather than a constraint on the nature of the objects considered, and (2) the number density of objects does not correspond to $(\delta T/T)^{-2}$ but to $(\delta T/\tau T)^{-2}$, which is a much smaller number if $\tau << 1$. In the particular form the model takes in this paper, physical processes associated with known astronomical objects with the required

number density are proposed to account for the optical depth demanded by the homogeneity of the background radiation on the angular scale of the measurements reported in this paper.

Observational evidence that intergalactic gas can produce an observable, small angular scale perturbation is the detection by Pariiskii (1972) of a 1.2 mK decrease in the background radiation temperature in the direction of the Coma cluster with a telescope of half-power beamwidth 22 arcmin. The implied optical depth is 4.4×10^{-4}, comparable to the estimated optical depth of ten scatterers in the model.

g) Entropy Fluctuations

Fluctuations in the number of baryons associated with a given number of photons of unperturbed density, unlike density perturbations, would not be subject to damping during the radiation-dominated era. Gott and Rees (1975) proposed a model in which the spectrum of baryon density fluctuations at recombination was

$(\delta\rho/\rho)_{b,rec} = 4.8 \times 10^{-3} \Omega 1/2\ M_{15}^{-1/3}$, normalized by fitting to Peebles' (1974) spatial covariance function. If we estimate

$$\frac{\delta T}{T} = \frac{1}{3} \left(\frac{\delta\rho}{\rho}\right)_{rec} e^{-\tau} \text{ and } \left(\frac{\delta\rho}{\rho}\right)_{rec} = \frac{\Omega}{\Omega + 1.45} \left(\frac{\delta\rho}{\rho}\right)_{b,rec},$$[11]

[11] The baryon density is equal to the photon density times $(1000/z)\Omega$; and the optical thickness of perturbations on all scales drops to unity at a redshift close to

$z = 1055$ (Sunyaev and Zeldovich 1970a). Therefore, at the epoch when baryon density perturbations could generate radiation fluctuations, baryons were approximately half of the total density. The photons were distributed strictly homogeneously by hypothesis, as were the neutrinos, which had a density 0.45 times the photon density.

and use Silk's (1974b) formula[12] for the optical depth to the redshift at which a given mass scale becomes transparent, then we find that $\delta T/T$ reaches a maximum of $2.4 \times 10^{-4}\ g(\mathcal{A})$, where $g(\mathcal{A}) \equiv 2.45\mathcal{A}^{5/3} / (1.45 + \mathcal{A}) \approx 1$, at an angular scale of $\theta = 1.22\,\mathcal{A}^{\frac{1}{2}}$ arcmin. This is 0.3 $g(\mathcal{A})$ times the limit on $\delta T/T$ at 1.25 arcmin reported in this paper.

If we had used Sunyaev and Zeldovich's (1970a) formula[13] for the optical depth, the peak $\delta T/T$ would be $1.76 \times 10^{-4}\ g(\mathcal{A})$ at $\theta = 3.3\mathcal{A}^{\frac{1}{2}}$ arcmin, which is 1.2 $g(\mathcal{A})$ times the observed upper limit on $\delta T/T$ at 3.3 arcmin. It seems that, unless the simple estimate of $\delta T/T$ is much too large, the observations are close to being able to test this theory.

h) Primordial Turbulence

Chibisov and Ozernoy (1969) evaluate the background temperature fluctuations for a model in which whirl motions with a Kolmogorov velocity spectrum[14] are postulated to account for the angular momentum of galaxies today. This model predicts inhomogeneities in the cosmic background radiation of $\delta T/T = 1.04 \times 10^{-3}\ \mathcal{A}^{5/4}\ e^{-\tau_i}$, where τ_i is the optical depth due to reionization, which was estimated to

---

[12] $\tau = 0.45 + 0.65\ (\mathcal{A}^{1/2}\ M_{15})^{-1/3}$

[13] $\tau = 0.4 + 1.9\ (\mathcal{A}^{1/2}\ M_{15})^{-1}$

[14] The velocities on different scales are related by $v_r \propto r^{1/3}$.

be 0.2 or less in a preceding section. The characteristic angular scale of the inhomogeneities would be $0.045\Omega^{5/3}$ arcmin = $2.6\Omega^{5/3}$ arcsec. The observational limit on $\delta T/T$ reported in this paper is 15 times the predicted inhomogeneity when extrapolated to 0.045 arcmin.

Silk and Ames (1972) consider the growth and damping of turbulence and conclude that it might generate density perturbations $\delta\rho/\rho$ of 0.01 to 0.1 at recombination on a mass scale of 10^{12} $M_\odot$. These would grow into galaxies with the required angular momentum at a $z < 10$ and would generate fluctuations $\delta T/T = 3.2 \times 10^{-5}$ on an angular scale of 0.2 arcmin, at which the observed limit is $\delta T/T \leq 4 \times 10^{-3}$. Stronger constraints are placed on primordial turbulence theories by the limit on the distortion of the blackbody spectrum by the dissipation processes (Zeldovich and Sunyaev 1969) than by the limits on the inhomogeneity of the radiation.

i) Interactions with Gravitational Waves

Gravitational waves are generated by density fluctuations and cause temperature fluctuations by causing a dispersion in redshifts between different regions emitting or scattering photons. The limit on large-scale density perturbations discussed above was obtained from the calculation of this effect by Sachs and Wolfe (1967), but, for masses less than 10^{18} $M_\odot$, scattering from the surface of

density fluctuations produces larger temperature fluctuations than the associated gravitational waves (Sunyaev and Zeldovich 1970a).

Gravitational waves also affect the cosmic background radiation in a manner similar to a medium with a random, inhomogeneous index of refraction (Dautcourt 1969). Pariiskii (1973a) has shown that the energy density of gravitational waves is less than $10^{-6}\rho_c$ on scales greater than 3 Mpc today, less than $0.1\ \rho_c$ on scales greater than 0.3 Mpc, and less than ρ_c for all scales greater than 50kpc, and that Thomson scattering by reionized gas cannot substantially change these conclusions. The observation in this paper confirms his extrapolation and reduces his limit by a factor of two for scales less than 0.15 Mpc. (The angular scale corresponding to 1 Mpc is 9 arcmin.)

V. CONCLUSIONS

The observations reported in this paper have set a new upper limit to the inhomogeneity of the cosmic background radiation on angular scales of 1.75 arcmin or less. The discrete source hypothesis for the origin of the cosmic background radiation has been shown to be untenable independently of the question of fitting the Planck blackbody spectrum. An optical depth comparable to unity for redshifts $z \ll 1000$ has been shown to be very unlikely. This has the double consequence that (1) if the intergalactic medium has been reionized, it occurred at a redshift less than 22, and (2) inhomogeneities introduced in the background radiation that survived the recombination era would be observable today not significantly diminished in amplitude. This permitted a direct comparison between observational limits on $\delta T/T$ and the predicted $\delta T/T$ in various theories about the origin of galaxies.

Clustering on scales larger than 100 Mpc is limited by the cosmic background inhomogeneity measurements to a maximum 10% increase in density, and direct observations confirm this to be the case. Density enhancements containing 10^{15} $M_\odot$ or more,[15] if they exist, are not expected to be gravitationally bound. Density and entropy fluctua-

[15] The maximum mass of gravitationally bound systems is less than 10^{15} $M_\odot$, but the rapidly increasing opacity to the redshift at which smaller perturbations become transparent prevents deriving the cutoff directly from the cosmic background observations.

tions on scales corresponding to the largest clusters of galaxies are marginally constrained by the observed limits on $\delta T/T$. Gravitational waves in the universe with wavelengths comparable to the spacing between galaxies or longer are restricted to have an energy density no greater than one-tenth of the Einstein-de Sitter density, which is consistent with the restrictions on the total density of the universe discussed at the beginning of Section IV.

The principal advantage of the limit on $\delta T/T$ reported in this paper is its small angular scale, comparable to the smallest perturbations which generate inhomogeneities in the background radiation that survive the recombination era. Although inhomogeneities in the radiation generated by perturbations with masses comparable to the mass of a galaxy would not survive the recombination era, protogalaxies might subsequently interact with the background radiation at the time that they collapse into galaxies; and at that redshift their angular separation is nearly equal to the angular scale of these observations. A simple model consistent with the observed number of galaxies and the observed limit on $\delta T/T$ is proposed for this interaction.

REFERENCES

Alexanian, M. 1970, Astrophys. J., 159, 745.

Bennett, C. A. and Franklin, N. L. 1954, Statistical Analysis in Chemistry and the Chemical Industry, (Wiley & Sons: New York), pp. 319 - 327, 349.

Boynton, P. E. and Partridge, R. B. 1973, Astrophys. J., 181, 243.

Carpenter, R. L., Gulkis, S. and Sato, T. 1973, Astrophys. J. (Letters), 182, L79.

Chibisov, G. V. and Ozernoy, L. M. 1969, Astrophys. Lett., 3, 189.

Conklin, E. K. and Bracewell, R. N. 1967a, Phys. Rev. Lett., 18, 614.

_____ 1967b, Nature, 216, 777.

Dautcourt, G. 1969, Astrophys. Lett., 3, 15.

Dent, W. A. and Kapitzky, J. E. 1975, (private communication).

Epstein, E. E. 1967, Astrophys. J. (Letters), 145, L157.

Gott, J. R., Gunn, J. E., Schramm, D. N. and Tinsley, B. M. 1974, Astrophys. J., 194, 543.

Gott, J. R. and Rees, M. J. 1975, Astron. Astrophys., 45, 365.

Layzer, D. and Hively, R. 1973, Astrophys. J., 179, 361.

Linsky, J. L. 1973, Astrophys. J. Suppl., No. 216, 25, 163.

Longair, M. S. and Sunyaev, R. A. 1969, Nature, 223, 719.

Nicolson, G. D. 1970, Trans. IEEE, MTT18, 169.

Pariiskii, Yu. N. 1972, Astron. Zh., 49, 1322, [Soviet Astron., 16, 1048, (1973)].

_____ 1973a, Astron. Zh., 50, 453, [Soviet Astron., 17, 291, (1973)].

_____ 1973b, Astron. Zh., 50, 673, [Soviet Astron., 17, 431, (1974)].

_____ 1973c, Astrophys. J. (Letters), 180, L47.

_____ 1974, Astrophys. J. (Letters), 188, L113.

Pariiskii, Yu. N. and Pyatunina, T. B. 1970, Astron. Zh., 47, 1337, [Soviet Astron., 14, 1067, (1971)].

Peebles, P. J. E. 1974, Astrophys. J. (Letters), 189, L51.

Peebles, P. J. E. and Yu, J. T. 1970, Astrophys. J., 162, 815.

Peimbert, M. and Torres-Peimbert, S. 1976, Astrophys. J., 203, 581.

Penzias, A. A., Schraml, J. and Wilson, R. W. 1969, Astrophys. J. (Letters), 157, L49.

Penzias, A. A. and Wilson, R. W. 1966, Astrophys. J., 146, 666.

Sachs, R. K. and Wolfe, A. M. 1967, Astrophys. J., 147, 73.

Sandage, A. and Tammann, G. A. 1975, Astrophys. J., 197, 265.

Silk, J. 1974a, Astrophys. J., 193, 525.

_____ 1974b, Astrophys. J., 194, 215.

Silk, J. and Ames, S. 1972, Astrophys. J., 178, 77.

Smith, M. G. and Partridge, R. B. 1970, Astrophys. J., 159, 737.

Stankevich, K. S. 1970, Australian J. Phys., 23, 111.

Sunyaev, R. A. and Zeldovich, Ya. B. 1970a, Astrophys. Space Sci., 7, 3.

_____ 1970b, Astrophys. Space Sci., 9, 368.

Troitsky, V. S. 1962, in IAU Sumposium No. 14, The Moon, Z. Kopal and Z. K. Mikhailov, eds., (Academic Press: New York), p. 475.

Wall, J. V. and Cooke, D. J. 1975, Monthly Notices Roy. Astron. Soc., 171, 9.

Webster, A. 1976, Monthly Notices Roy. Astron. Soc., 175, 61.

Weedman, D. W. 1976, Astrophys. J., 203, 6.

Wolfe, A. M. and Burbidge, G. R. 1969, Astrophys. J., 156, 345.

Woody, D. P., Mather, J. C., Nishioka, N. S. and Richards, P. L. 1975, Phys. Rev. Lett., 34, 1036.

Zeldovich, Ya. B. and Sunyaev, R. A. 1969, Astrophys. Space Sci., 4, 301.

FIGURE 1

System temperature including dry-weather atmospheric contribution as a function of telescope zenith angle (boxes) and of the secant of the zenith angle (circles). Solid points refer to spring 1975 observations; open points refer to fall 1974 observations and have been increased 4 K (cf. section II d in text). The zenith angle range observed on each date is listed in Table 1.

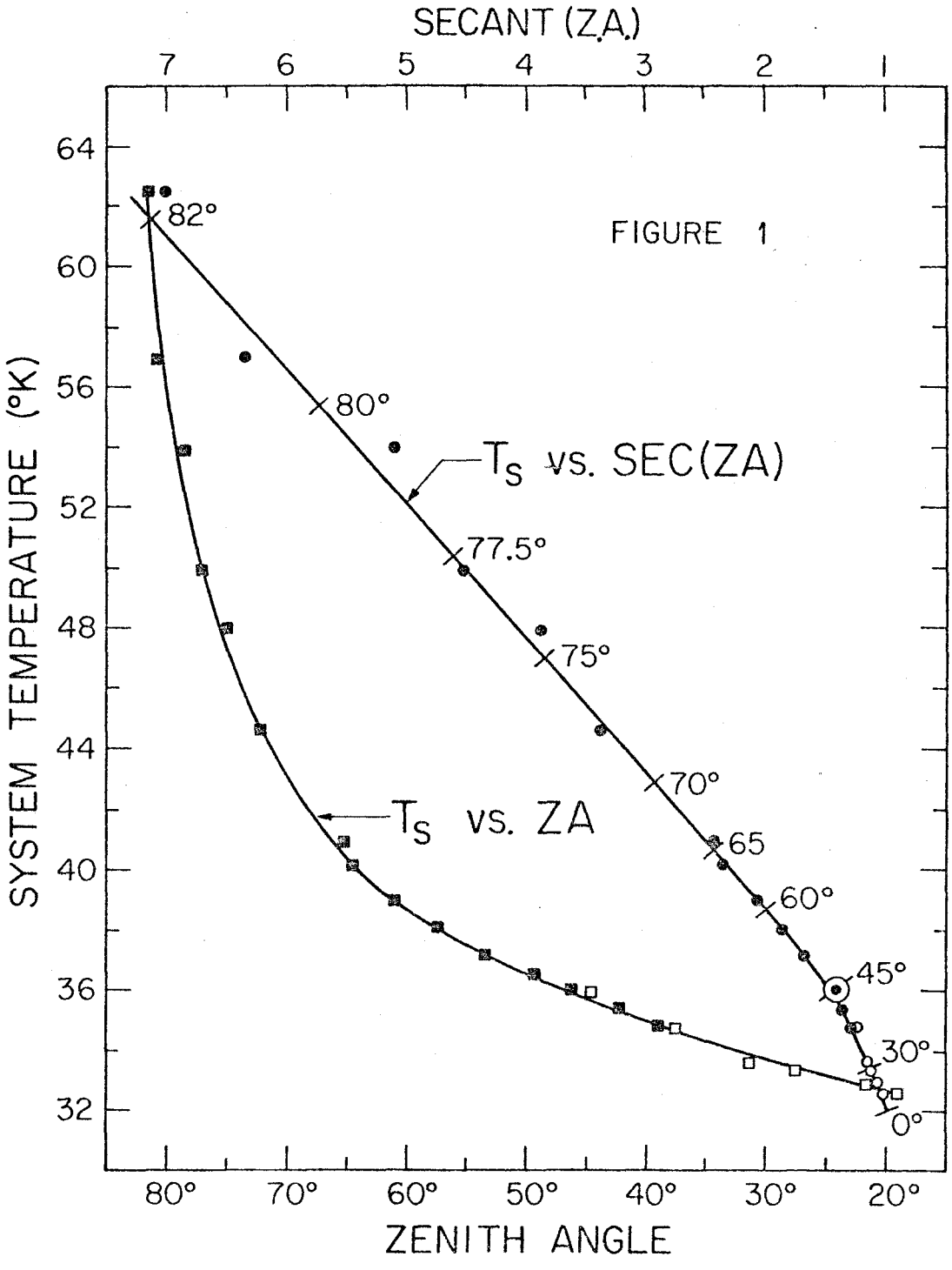
SECANT (Z.A.)
7
6
5
4
3
2
1
64
60
56
52
48
44
40
36
32
SYSTEM TEMPERATURE (°K)
82°
80°
77.5°
75°
70°
65
60°
45°
30°
0°
T_S vs. SEC(ZA)
T_S vs. ZA
80°
70°
60°
50°
40°
30°
20°
ZENITH ANGLE

FIGURE 1

FIGURE 2

The mean scan. Bars represent the antenna temperature in one-beamwidth cells averaged over 448 scans of the selected region. A linear baseline (not shown) has been subtracted from the data. Horizontal lines indicate ± one standard deviation of a cell (0.95 mK). Solid points represent antenna temperatures that have been roughly corrected for spillover from adjacent cells (cf. section III d in text). The Gaussian and the sloping baseline illustrate the contribution of a hypothetical 15 mJy source to the antenna temperatures (cf. section III c in text). Open points are the source contribution averaged over each cell.

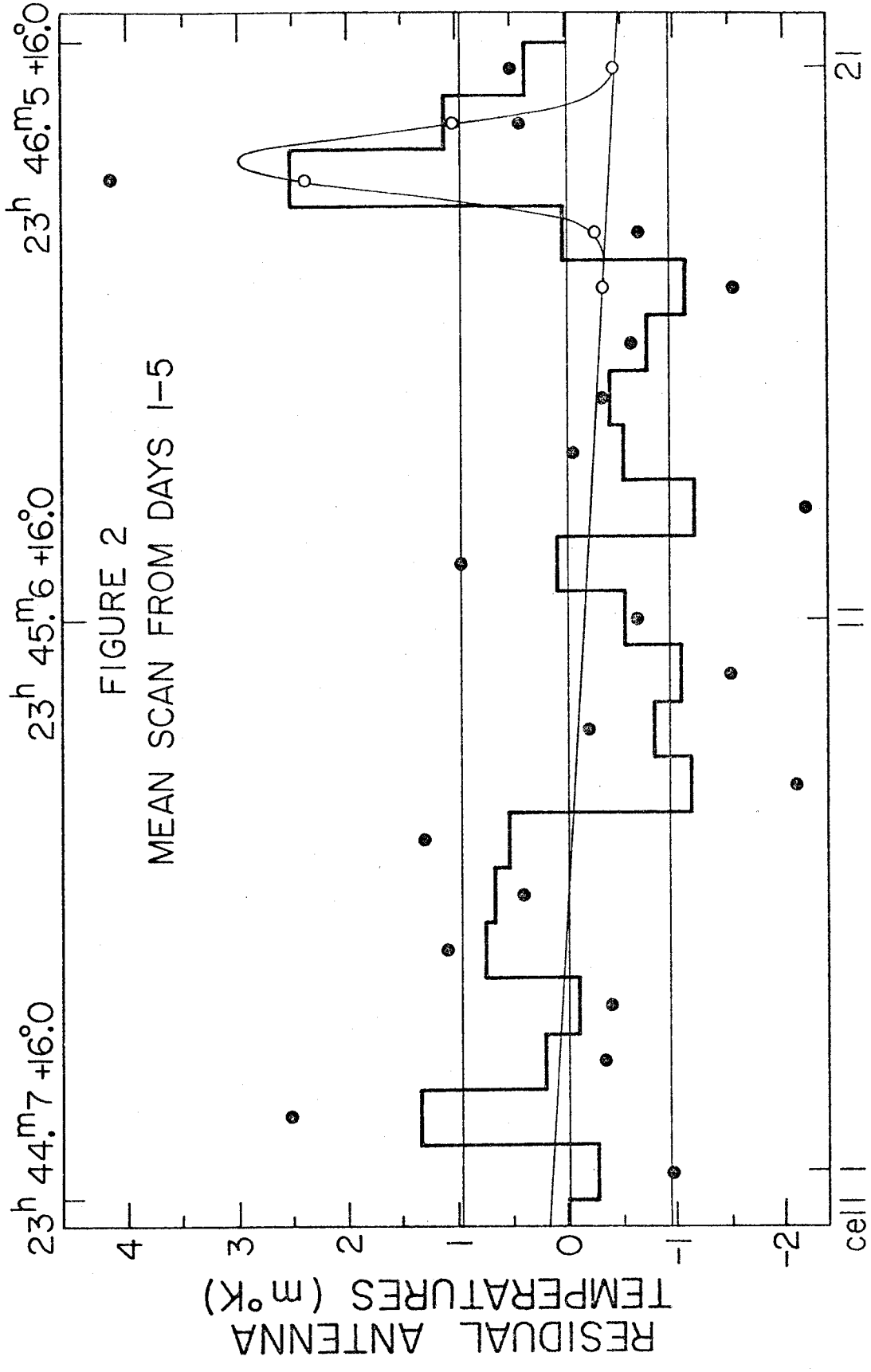

FIGURE 2
MEAN SCAN FROM DAYS 1–5

FIGURE 3

Variance of antenna temperatures in one-beamwidth cells in a mean scan vs. the reciprocal of the number of scans integrated to form that mean scan. The solid line shows the least squares fit to Equation (4). The horizontal line indicates the upper limit at the 95% confidence level to the asymptotic value as the number of scans becomes infinite ($n^{-1} = 0$). Numerical values are supplied in Tables 2 and 3. Error bars indicate $\pm$ one standard deviation of the plotted points. The significance of the solid points and the open points is discussed in section III c of the text. The points for a single scan (n = 1) have been plotted at 1/6 of their true abscissa and ordinate values in order to avoid crowding the other points.

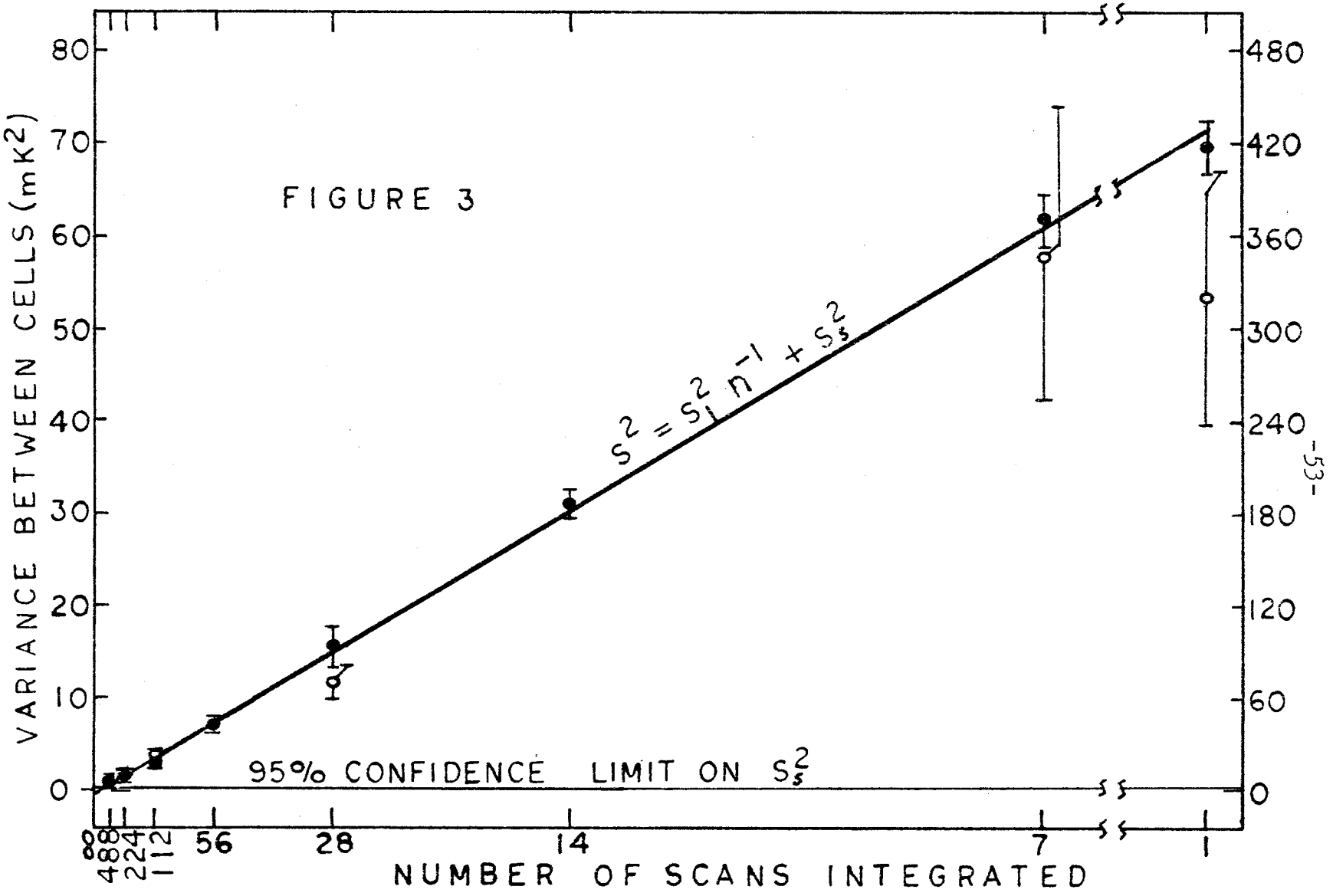
FIGURE 3
VARIANCE BETWEEN CELLS (mK²)
80
70
60
50
40
30
20
10
0
480
420
360
300
240
180
120
60
0
$S^2 = S_1^2 n^{-1} + S_s^2$
95% CONFIDENCE LIMIT ON S_s^2
488
224
112
56
28
14
7
1
NUMBER OF SCANS INTEGRATED

FIGURE 4

Upper limit on root-mean-square background temperature fluctuations as a function of angular scale. The solid curve is the extrapolation of the limit reported by this paper (2.00 mK at 1.25 arcmin) by Equations (5) and (6). The dashed line is the locus of possible observations which would extrapolate to that limit by Equation (5). Limits obtained by other observers are also plotted; they are identified in Table 4. Triangles indicate observations made at 3.5 mm wavelength; all other observations were made at wavelengths from 2 to 4 cm. The circle indicates the confusion level estimated in section III c.

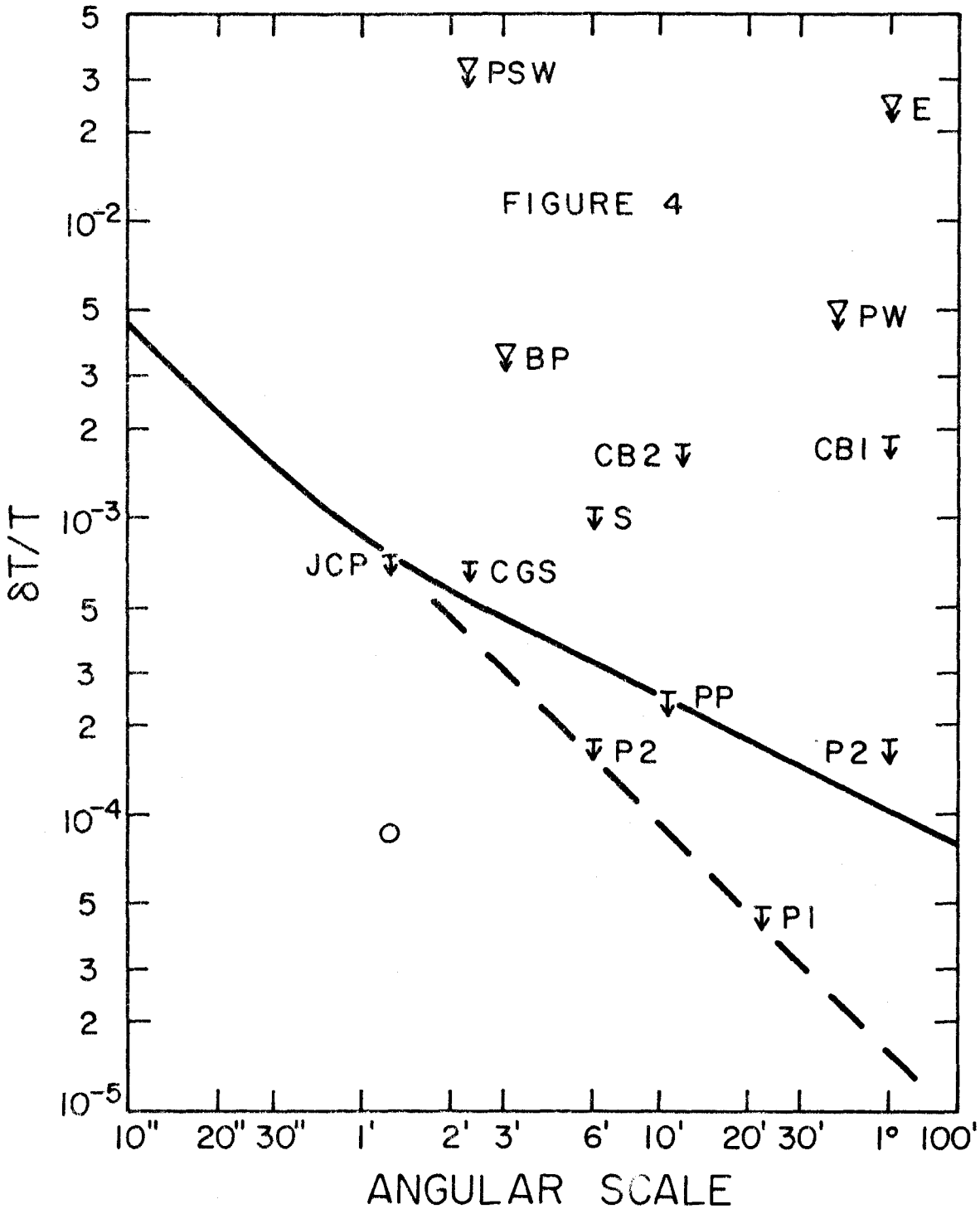
PSW
E
PW
BP
CB2
CB1
S
JCP
CGS
PP
P2
P2
P1
δT/T
ANGULAR SCALE
10"
20"
30"
1'
2'
3'
6'
10'
20'
30'
1°
100'

FIGURE 4

APPENDIX A

Angular Sizes

The angular size of an object with diameter L seen at a redshift z in an expanding Friedmann universe with zero cosmological constant is given by (e.g. Sandage 1961, Mattig 1958)

$$\theta(L,z) = \frac{L}{cH_o^{-1}} \; f(\Omega,z), \text{ where}$$

$$f(\Omega,z) \equiv \frac{\frac{1}{2}\Omega^2 (1+z)^2}{\Omega z+(\Omega-2)(\sqrt{1+\Omega z}\;-1)} \qquad \text{(A1)}$$

The function f has a minimum value ≈ 2 at $z \approx 3$ (cf. Table 6), and asymptotic behavior

$$f \approx z^{-1} + 1.5 \qquad (z < 1)$$

$$2.8 < f < 3.0 \qquad (\Omega z = 1,\ \Omega < 0.6)$$

$$f \approx \Omega z/2 \qquad (\Omega z >> 1) \qquad \text{(A2)}$$

If the object is a sphere containing a mass M at the average density of the universe, L depends on redshift

$$L(M,z) = (6M/\pi\Omega\rho_c)^{1/3} \; (1+z)^{-1} \qquad \text{(A3)}$$

Using the definition of the critical density in an Einstein-deSitter universe $\rho_c = 3H_o^2/8\pi G$, we have

$$\theta(M,z) = (16GM)^{1/3} c^{-1} H_o^{1/3} \Omega^{-1/3} (1+z)^{-1} f(\Omega,z) \qquad \text{(A4)}$$

and

$$\theta(M,z) \approx (16GM)^{1/3} c^{-1} H_o^{1/3} \Omega^{-1/3} (z^{-1}+0.5) \quad (z < 1)$$

$$\theta(M,z) \approx (16GM)^{1/3} c^{-1} H_o^{1/3} \Omega^{2/3} (z^0/2) \quad (\Omega z >> 1) \qquad \text{(A5)}$$

The minimum $\theta(M,z)$ occurs not at $z \approx 3$ but when $\Omega z >> 1$.

TABLE 6

SOME MINIMA OF THE ANGULAR DIAMETER FUNCTION $f(\Omega, z)$

DENSITY Ω	REDSHIFT z at f_{min}	f_{min}	MIN. ANGLE IN ARCMIN* SUBTENDED BY 1 Mpc.
0.02	5.11	2.14	1.36
0.05	3.66	2.25	1.43
0.1	2.83	2.38	1.51
0.2	2.20	2.56	1.62

*For $H_o = 55$ km s^{-1} Mpc^{-1} = $(1.77 \times 10^{10}$ yrs$)^{-1}$, $cH_o^{-1} = 5427$ Mpc.

LITERATURE CITED IN APPENDIX A

Mattig, W. 1958, Astronomishe Nachrichten, 284, 109.

Sandage, A. 1961, Astrophys. J., 133, 355.